A NEW APPROACH FOR REAL-TIME FAULT DIAGNOSIS IN INDUCTION MOTORS BASED ON A DIGITAL SIGNAL PROCESSOR EMBEDDED IN FPGA

Cesar da Costa [1]
Mauro Hugo Mathias [2]

Data de entrega dos originais à redação em: 24/11/2014
e recebido para diagramação em: 19/05/2016.

This paper proposes a new approach for the design of a real-time vibration measurement and analysis instrument based on a digital signal processor embedded in a field-programmable gate array (FPGA). Circuit architecture mapped from a MATLAB/SIMULINK model is the main idea in this new approach. Signal processing algorithms, such as FIR filters, fast Fourier transform, and the high-frequency resonance technique, are implemented in hardware embedded in the FPGA using a system generator toolbox. This automatically translates the MATLAB/SIMULINK model into a hardware description language, VHDL. Special focus is dedicated to the area of fault detection in rolling bearings.

Keywords: Rotating Electrical Machine. Fault. Condition Monitoring. Diagnostic. Vibration. Digital Signal Processing.

1 INTRODUCTION

Machine vibration analysis has become an important tool for the identification of machine faults. Large electromechanical systems are often equipped with sensors of mechanical quantities. In many situations, vibration monitoring methods are used to detect the presence of incipient failures, and it has been proposed that stator current monitoring can provide the same indications without requiring access to the motor [1]. In this context, various sensors can be used to collect measurements from a rotating machine for the purpose of condition monitoring. These sensors can measure stator voltages and currents, air-gap and external magnetic flux densities, rotor position and speed, output torque, internal and external temperature, and case vibrations, among others. A real-time vibration measurement and analysis instrument can monitor a variety of possible failures. For the purpose of detecting such fault-related signals, many diagnostic methods have been developed. These methods to identify faults in rotating machines may involve several different types of fields of science and technology [2, 3].

According Benbouzid [1] and Sadoughi et al. [2] analysis can be divided into two types: in the time domain and in the frequency domain. Frequency domain analysis can give more detailed information about the status of the machine. Time domain analysis can give qualitative information about the machine condition. Traditionally, fast Fourier transform (FFT) was used to perform frequency domain analysis.

Al Kazzas et al. [4] investigated induction machine condition monitoring and fault diagnosis using digital signal processing techniques. Different methodologies based on vibration spectral analysis have been proposed using fast Fourier transform (FFT) [5], [6], and [7]. In the last decade, real-time vibration measurement and analysis instruments have become one of the important tools for machine fault identification [8], [9]. Historically, vibration monitoring techniques have been widely used for the diagnosis of faults in induction motors, but, as reported by Lebaroud et al. [15], electrical detection methods have been preferred in recent years. Nevertheless, all of the presently available techniques require the user to have some degree of expertise to distinguish a normal operating condition from a potential failure mode. This happens because the monitored spectral components can result from a number of sources, including those related to normal operating conditions [6], [7].

Embedded systems have grown tremendously in recent years, not only in their popularity but also in their complexity. The modelling of instrumentation systems requires the use of a set of tools to obtain a simulation of physical systems. For design engineers, these tools should enable the design of a simplified physical model, as close as possible to the real model, allowing its implementation in real time and within the required levels of accuracy [7], [9] and [11]. This complexity increases the demands on the system developer that must work in the hardware design as well as in the software design.

FPGAs offer ample quantities of logic and register resources that can easily be adapted to support the fine-grained parallelism of many pipelined digital signal processing applications. With current logic capacities exceeding one million gates per device, substantial logic functionality can be implemented on each programmable device [6], [8].

This paper presents a new approach to the development of a real-time vibration measurement instrument that uses the analysis of vibration signals to enhance detectability for mechanically unloaded operating conditions of the rotating machine that other isolated techniques are unable to detect. Special purpose digital signal processing (DSP) hardware, implemented into a FPGA, is developed to provide on-line detection, measurement, and analysis that do not require the diagnosis of a highly trained expert technician to estimate the motor condition [6], [7].

1 - Faculty of Engineering, Department of Mechanical - UNESP - Universidade Estadual Paulista Julio de Mesquita Filho Guaratingueta, São Paulo, Brasil. < cost036@hotmail.com >.
2 - Faculty of Engineering, Department of Mechanical - UNESP - Universidade Estadual Paulista Julio de Mesquita Filho Guaratingueta, São Paulo, Brasil. < mathias@feg.unesp.br >.

MATLAB/SIMULINK was used for prototyping the digital signal processing application in terms of functional blocks, and the respective simulation. The DSP Builder software tool was used within SIMULINK to support the design and direct compilation of the digital signal processing routines to the FPGA [7], [8], [11] and [12].

2 MODELING THE INSTRUMENT FOR VIBRATION MEASUREMENT AND ANALYSIS

The development of an instrument for vibration measurement and analysis for the identification of machine faults is described. In the first stage, the overall measurement and analysis system model was developed in MALAB and its SIMULINK toolbox. In the second stage, the model of the analysis algorithms was modeled in DSP Builder software and converted to VHDL code. The design was captured and presented in a way that allows the VHDL code to be generated automatically [6, 7].

SIMULINK is a dynamic system and simulation software that offers an interactive scientific and engineering environment for system modeling, analysis, and simulation [9]. This environment is useful for the rapid implementation of a digital signal processing application in terms of functional blocks, and provides high-level simulation capabilities. A functional block is a basic structure that can represent a function or a specialized system, with well-defined input and output ports and customized parameters. In this paper, the focus is centered on the implementation and testing of algorithms using block diagrams for data flow modeling for an instrument for vibration measurement and analysis. SIMULINK uses a set of libraries for signal processing to represent dynamic systems [9, 10]. The standard block library is organized into several subsystems, i.e., grouping blocks, according to their behavior. In practice, the system developer must map the behavior of electronic hardware to symbolic representation in SIMULINK. The next subsections present the SIMULINK model of vibration measurements and analysis instrument.

a) Data acquisition and filter model

The sensor used for the data acquisition of motor vibration was the accelerometer B&K, model 4371, with sensitivity of 9.77 pC/g, mounted on the motor structure. The output vibration signal from the accelerometer was amplified and conditioned by an instrument model 133 from Endevco. The output signal conditioner was connected to the input of a data acquisition board, model NI USB-9234 from National Instruments with four analog input channels, a 24-bit resolution and a maximum acquisition rate of 51.2 kS/s.

The data acquisition and filter model consisted of one analog input block to drive the signal sensor, a subsystem of linear scaling of the signal, a low-pass 6th order Butterworth filter with a cut-off frequency of 12 kHz, and a subsystem of high pass filters. The filters are used for two purposes: to attenuate the noise and undesired frequency components and to separate some individual frequencies or band of frequencies for their relation with the machine faults [7, 4]. The model display produces a time domain graphic of amplitude versus time of the input signal. Figure 1 shows the functional block representing the data acquisition and filter model.

b) Time domain analysis model

The simplest approach in the time domain is to measure the overall root-mean-square (RMS) value, peak value, and crest factor (ratio of peak value to RMS value) of the vibration signal. Some statistical parameters of the vibration signal, such as probability density function and kurtosis, have been proposed for bearing defect detection [4]. The probability density function of the acceleration of a bearing in good condition has a Gaussian distribution; for a damaged bearing it has a non-Gaussian distribution with dominant tails because of a relative increase in the number of high levels of acceleration [13]. Instead of studying the probability density curves, it is often more informative to examine the statistical moments of the data. The first and second moments are well known, as they are the mean value and the variance, respectively. The third moment, normalized with respect to the cube of standard deviation, is known as the coefficient of skewness. The fourth moment, normalized with respect to the fourth power of standard deviation, is quite useful and is called kurtosis [13]. The time domain analysis model consists of one subsystem of time domain analysis block and a multiport switch. Signal analysis is used to extract some useful features of the signal, i.e., RMS value, peak value, crest factor, and kurtosis. The numeric display of the model shows the value

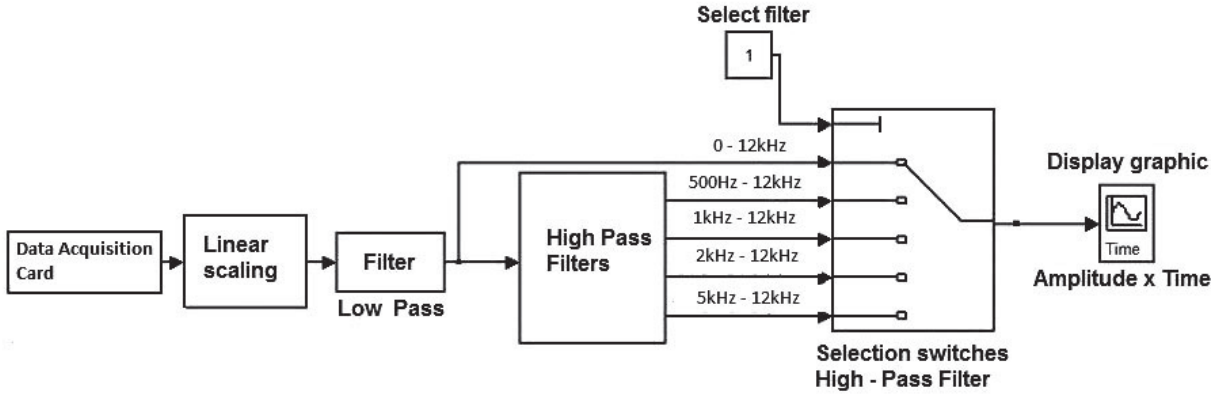

Figure 1 - Schematic diagram of the data acquisition and filter model

of the variable selected by the multiport switch. Figure 2 shows a functional block representing the time domain analysis model.

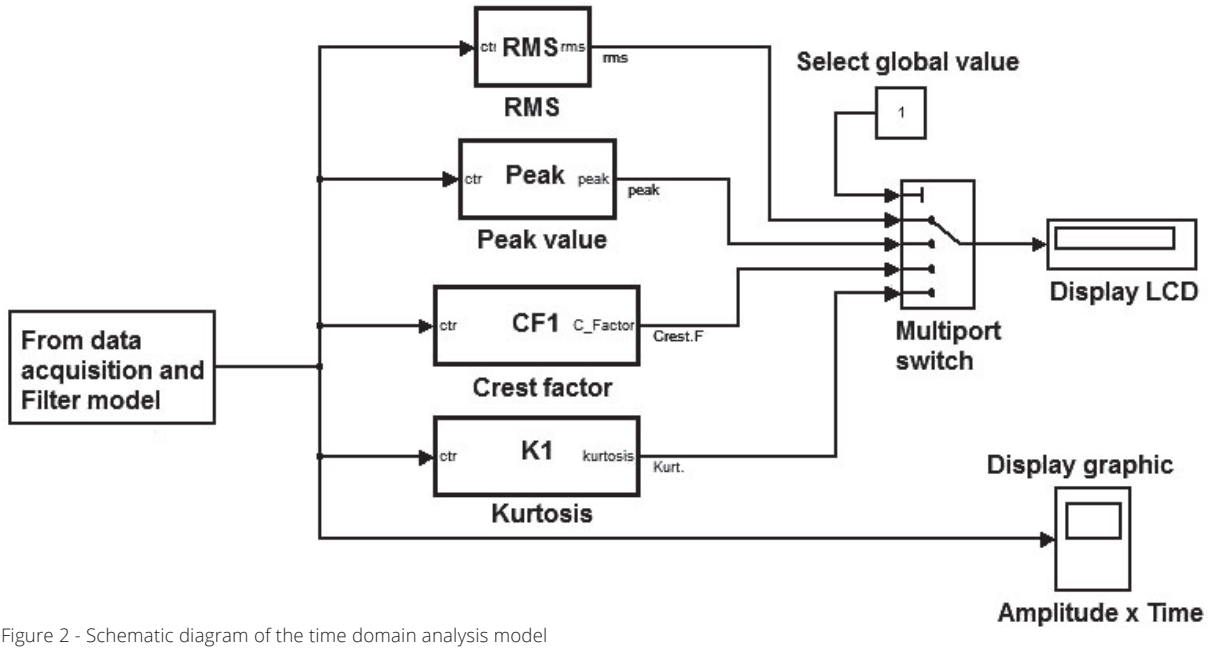

Figure 2 - Schematic diagram of the time domain analysis model

Figure 3 shows the vibration signal in the time domain. Figure 3(a) corresponds to a motor without fault while Figure 3(b) corresponds to a motor with bearing fault. Both graphics were obtained with the model implemented in Figure 2. Note that, in the time domain, information about failures is not detailed in the graphics. For more information on time domain analysis a new vibration severity measurement model is needed.

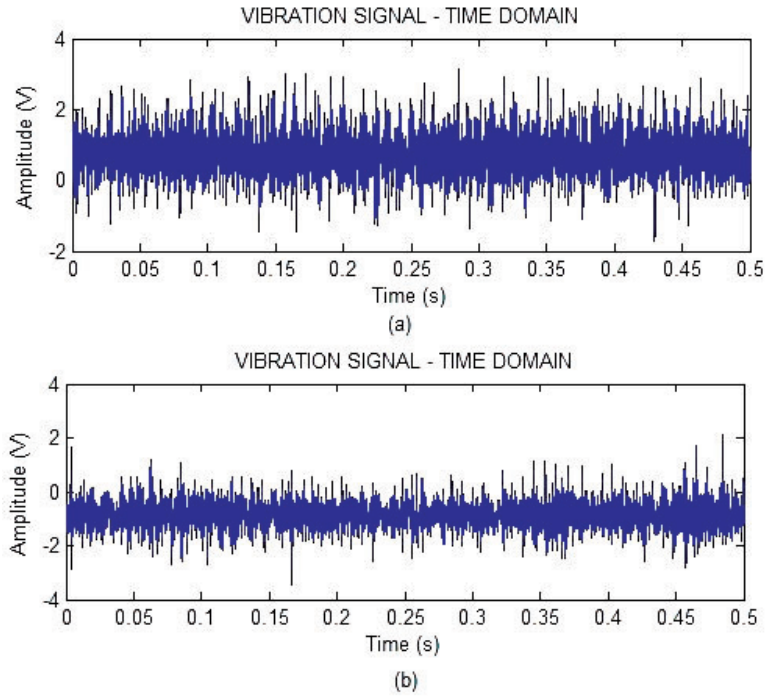

Figure 3 - Vibration signal in the time domain. Motor without fault (a) and motor with bearing fault (b)

c) Vibration Severity Measurement Model

Local defects can be detected in the time domain by displaying the vibration severity alarm due to the overall RMS level specified by vibration severity ISO 10816 -1 (former ISO 2372) [14]. A common procedure for monitoring the imbalance of rotating machines is the measurement of the RMS value of vibration, or the so-called vibration severity, which is a measurement of the energy of the emitted vibration [5]. The vibration severity is related to machine power class and running speeds. There are four power classes according to machine sizes and power ratings [14].

The vibration severity measurement model consists of one subsystem of vibration severity measurement block and four displays of machine status. Signal analysis is used to extract vibration severity measurement as specified by ISO Standard 10816-1, class I, and small machines. The model uses a routine developed in MATLAB that determinates the symptoms of machine status: good, satisfactory, unsatisfactory, and unacceptable [4, 5].

d) Critical Alarms Model

Large values of kurtosis indicate large peak values in the vibration signal. Different defects in a bearing produce high peak impulses, which have high frequency components. The RMS value and kurtosis, peak value, and crest factor are good indicators to distinguish between healthy and defective bearings, but none of them determines the type of fault [13]. For an undamaged bearing

with Gaussian distribution in the vibration signal, the kurtosis value is close to 3. A value higher than 3 is critical and is judged by itself to be an indication of impending failure and no prior history is required. In the same way, peak values in the time series signal will result in an increase in the crest factor value. For normal operations, the peak value can be between 3.8 mm/s and 15 mm/s and the crest factor between 2 and 6. A peak value above 15 mm/s and crest factor above 6 are critical and associated with machinery problems [13]. The critical alarms model consists of one subsystem of critical alarms block and three displays for alarms status. The model display shows the critical alarm when the value peak is larger than 15 mm/s, crest factor is larger than 6, and kurtosis is larger than 3.

e) Frequency Domain Analysis Model

Frequency domain or spectral analysis of the vibration signal is perhaps the most widely used approach in machine fault identification. The use of FFT analysis makes the job of obtaining narrowband spectra more efficient [4, 13]. Both low- and high-frequency ranges of the vibration spectrum are of interest in assessing the condition of the machine. RMS measurements in specific bands of frequency are used to derive an initial estimative about the status of the machine. The RMS value of these bands is used to specify the degree and the origin of the faults by comparing them with the corresponding RMS values in the bands of the reference spectrum and the knowhow of where each type of fault causes an increase in the RMS value [4]. From the literature and experimental observations, four frequency bands are selected to cover the vibration harmonics of mechanical and electromagnetic origin [4, 5, 15, and 13]. The frequency domain analysis model consists of normalization block, low pass filter block, and the FFT calculation block. The FFT is implemented in MATLAB. The model display produces a graph of amplitude versus frequency of the band frequency of the input signal. Figure 4 shows a functional block representing the frequency domain analysis model.

Figure 5 shows the vibration signal in the frequency domain. Figure 5(a) shows the vibration signal spectrum of a motor without fault while Figure 5(b) shows the equivalent for a motor with bearing fault. Both spectrums were obtained with the model implemented in Figure 4. To compare the overall level of vibration, the area under the curve was analyzed. The greater this area, the larger the global level of vibration will be. A comparison of Figure 5(a) and Figure 5(b) shows an overall vibration level higher in Figure 5(b), but no condition to identify what caused this increase in energy.

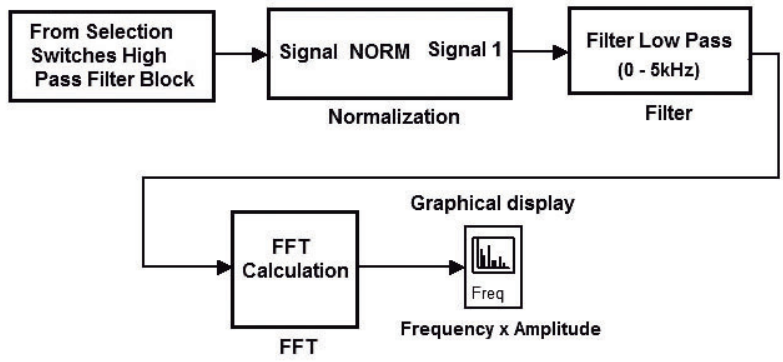

Figure 4 - Schematic diagram of the frequency domain analysis model

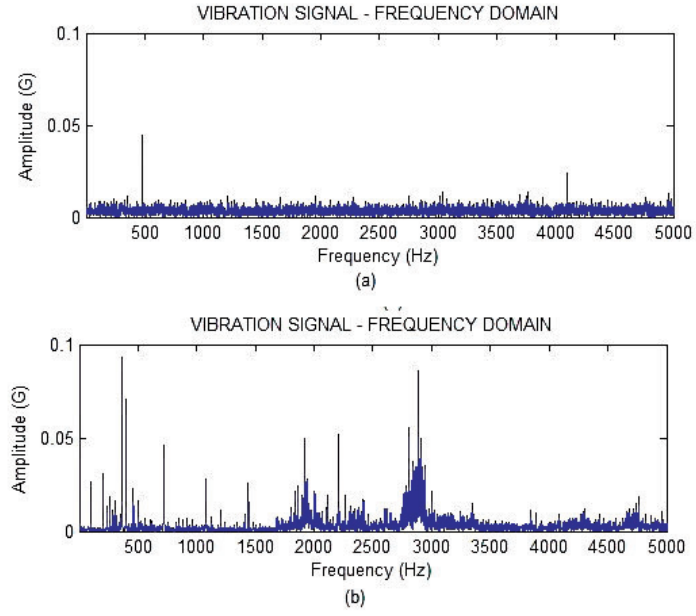

Figure 5 - Vibration signal in the frequency domain. Motor without fault (a) and motor with bearing fault (b)

3 APPLICATION TO ROLLING BEARINGS FAULTS

This section presents a case study to highlight the proposed design flow. The common faults of rolling bearings include corrosion in inner race, outer race and rolling elements, fatigue pitting, and cage damage. Any fault of inner race, outer race, and rolling elements will cause a modulation phenomenon. If there is a fault in either inner or outer race or rolling elements, mechanical impulses with higher amplitudes will occur while the shaft is rotating. These impulses will change the natural frequency of inner, outer race, and rolling elements [16, 17]. Each type of failure produces its own characteristic frequencies; these frequencies are related to the geometry of the bearing, the shaft speed, and location of the fault.

a) Geometry

For a particular bearing geometry, the inner race, outer race, and rolling element faults generate vibration spectra with unique frequency components. These frequencies, known as the fault frequencies, are functions of the running speed of the motor and the pitch diameter to ball diameter ratio of the bearing. Outer and inner race frequencies are also linear functions on the number of balls in the bearing. Given the geometry of the bearing

shown in Figure 6, Table 1 presents the four characteristic frequencies for an angular contact ball bearing in which the inner race rotates and the outer race is stationary. When the outer race is fixed, f_i is the rotation frequency of the shaft, D is the pitch diameter, d is the ball diameter, a is the contact angle, and z is the number of balls. It is assumed that the contact between balls and inner race and outer race is a pure rolling contact [18].

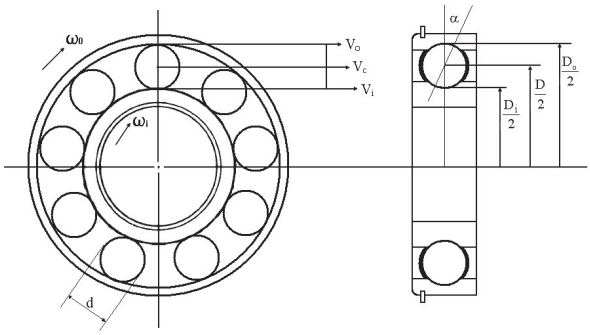

Figure 6 – Ball bearing geometry

Table 1 - Characteristic fault frequencies

Fault frequency of inner race	$f_{bi} = f_i \times \frac{Z}{2}\left(1+\frac{d}{D}\cos\alpha\right)$
Fault frequency of outer race	$f_{bo} = f_i \times \frac{Z}{2}\left(1-\frac{d}{D}\cos\alpha\right)$
Fault frequency of rolling elements	$f_{bs} = f_i \times \frac{D}{2d}\left[1-\left(\frac{d}{D}\right)^2\cos^2\alpha\right]$
Fault frequency of cage	$f_c = f_i \times \frac{1}{2}\left(1-\frac{d}{D}\cos\alpha\right)$

b) Faults Identification Approaches

Some works have used higher-order spectra to detect the fault frequency from modulated frequencies [16, 17]. This approach is useful when there is a simple modulation. However, in complex modulations it is hard to get a good result with this method. Thus, a virtual instrument system consisting of three stages is proposed: (i) 1st stage: the resonance frequencies characteristic of bearing failures, calculated theoretically; (ii) 2nd stage: analysis of the time domain to measurement the RMS value, peak value, crest factor, and kurtosis; (iii) 3rd stage: analysis of high-frequency resonance (the envelope technique – high-frequency resonance technique, or HFRT) in the frequency domain to identify the frequency of failures (peak values of the spectrum). Figure 7 shows the graphical representation of the virtual instrument system implemented [8].

In the first stage, the theoretical fault frequencies are calculated using the geometric data of the rolling bearing. In the analysis in the time domain (second stage) a computer routine measures parameters that demonstrate the existence of faults in rolling bearings, such as RMS value, peak value, crest factor, and kurtosis.

The interaction of the defect in the rolling element bearings produces pulses of very short duration, whereas the defect strikes the rotation motion of the system. The pulses excite the natural frequency of the bearing elements, resulting in the increase in the vibration energy at these high frequencies. The fault frequencies can be calculated theoretically. Each bearing element has a characteristic rotational frequency. With a defect on a particular bearing element, an increase in the vibration energy at this element rotational frequency may occur [19, 20, 21]. This defect frequency can be calculated from the geometry of the bearing and element rotational speed. By using HFRT, or the envelope technique, these frequencies can be isolated and demodulated to give an indication of bearing condition [19, 20, 21]. The envelope detection process is the heart of the HFRT diagnostic system. An accelerometer signal entering the envelope detector may be either attenuated or pre-amplified. The resulting signal is then sent through a band pass filter set for an appropriate carrier frequency. The filtered signal is then rectified and demodulated to extract the envelope of the modulated carrier frequency signal. This envelope is then analyzed for frequency content using a real-time frequency spectrum analyzer. The amplitude of the defect frequencies can be used to diagnose the condition of the rolling element bearing. In this work the five largest amplitude peaks of the spectrum to locate the frequency of fault (third stage) were identified. The experimental procedure was performed so that the virtual instrumentation system acquired data at a frequency of 10 kHz, during 4 seconds, comprising a total of 40000 samples for processing and analysis by the developed computer routines. Bearing model NSK 6205 was used to test, with previously known faults. The bearings were classified by the manufacturer according to the location of the fault (inner and outer race). Table 2 shows the geometric data of the NSK 6205 bearing used for the theoretical calculations of the frequency characteristics of bearing failures [8].

Table 2 - Geometrical parameters of the NSK 6205

Geometrical Parameters	Value
Number of balls	9
Ball diameter	7.96 mm
Inner raceway diameter	31.04 mm
Outer raceway diameter	46.72 mm

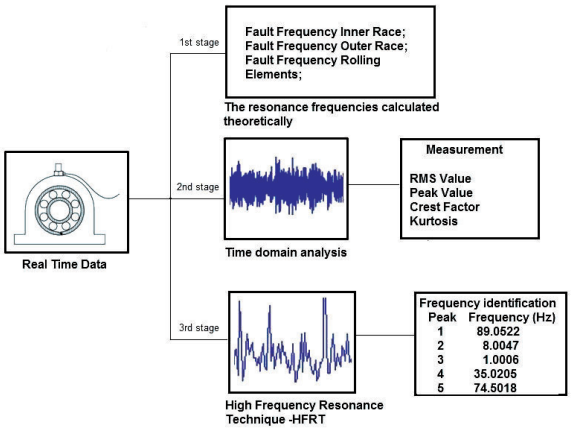

Figure 7 - Schematic diagram of the virtual instrument system

c) Prototype Setup

A laboratory setup was prepared to examine the theoretical results, which focused on the development and testing of algorithms and methods suitable for on-line detection of rolling bearing faults identification. A test bench was created to provide a representative model of a real situation where the bearing could be mounted in its housing and the active forces and velocities were similar to those found in actual situations of the industrial environment. The vibration sensor was an accelerometer with a bandwidth of more than 10 kHz. Figure 8 shows the setup of the test environment used for the development of computational algorithms for virtual instrumentation. Basically, it consists of a computer, a data acquisition board, an amplifier and signal conditioner, an accelerometer, and a three-phase induction motor.

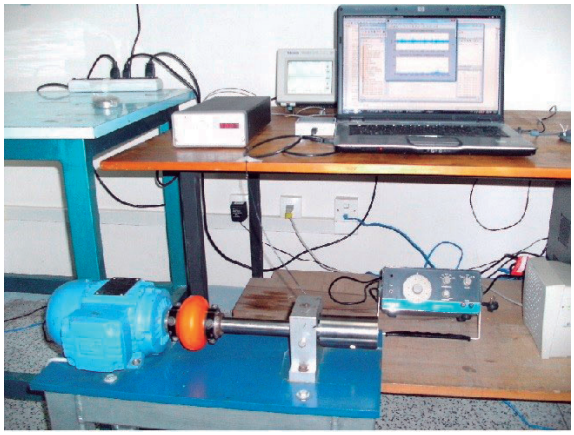

Figure 8 - Setup for bearing and related motor

d) Implementation of Virtual Instrument System Embedded in FPGA Hardware

The libraries of the functional blocks of the SIMULINK/DSP Builder software allowed the construction of the basic structure of the functional virtual instrumentation system. Figure 7 shows how this was divided into three stages.

A general purpose FPGA with an embedded soft-processor was chosen to maintain the reconfigurable fabric uncommitted for any particular function, thus opening room for the evaluation with different heterogeneous implementations. In addition, the fast reconfiguration feature of FPGAs may also be used to select among different digital systems according to the special requirements of a given task. The FPGA core board is the most important component of the embedded system. In this case study, an Altera DE2 board, represented in Figure 9, was used. The relevant features on the board are (i) SRAM with 512 kbytes, (ii) flash memory with 4 Mbytes, and (iii) 2 Mbits of block RAMs in the FPGA.

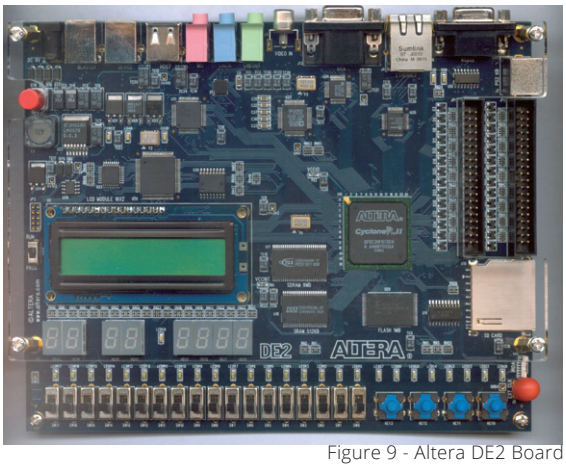

Figure 9 - Altera DE2 Board

After the graphic model is verified without error in the MATLAB/SIMULINK software, the DSP Builder software is operated to transform the model into VHDL language. The designed model files are analyzed and the model files are then transformed into general hardware description language files for the selection of chip type and clock cycle. After the hardware description files based on register transfer level (RTL) are acquired, the DSP Builder software will automatically complete integration, adaptation, and timing analysis. Finally, the files for download to the FPGA are generated. The working condition of actual circuit is consistent with the simulation results, reaching the design requirements.

e) Modelling Virtual Instrument System in SIMULINK/DSP Builder Software

Figure 10 shows the block diagram of the first stage of the instrument modelled in SIMULINK/DSP Builder software. The model consists of three subsystems: (i) calculation of inner race fault frequency, (ii) calculation of outer race fault frequency, and (iii) calculation of rolling element fault frequency.

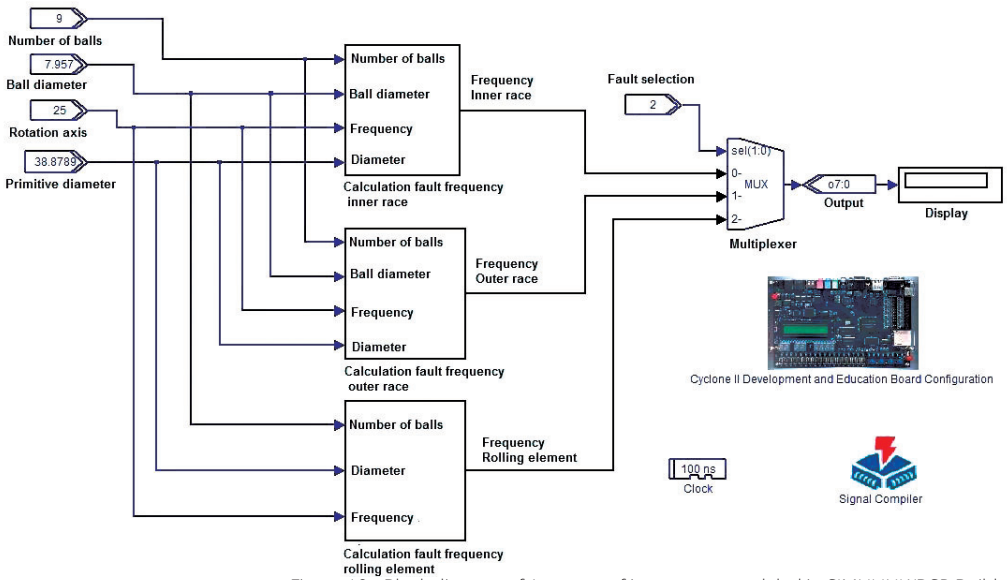

Figure 10 - Block diagram of 1st stage of instrument modeled in SIMULINK/DSP Builder

Figure 11 shows the block diagram of the second stage of the instrument modeled in the SIMULINK/DSP Builder software. The model consists of (i) calculation of the root mean square (RMS) value, (ii) calculation of the peak value, (iii) calculation of the crest factor, and (iv) calculation of the kurtosis. The numeric display shows a global value of the variable selected by the multiplexer block.

Figure 12 shows the block diagram of the third stage of the instrument modelled in the SIMULINK/DSP Builder software. The model consists of (i) normalization of the signal of vibration block, (ii) low pass filter block, (iii) the HFRT block, and (iv) the scope block that indicates the five largest amplitude peaks of the spectrum to locate the frequency of bearing fault.

f) Experimental Results

Table 3 shows the fault frequencies and harmonics calculate by the first stage of the instrument embedded in the FPGA, considering the rotation axis as 25 Hz (1500 rpm) and the geometric parameters of the NSK 6205 bearing (Table 2).

A Figure 13 shows the results obtained in the calculation of statistical parameters in the time domain in the second stage of the instrument embedded in the FPGA, with a fault bearing inner race.

Table 3 - Characteristic frequencies of bearing failures

Fault frequency (Hz)	Fundamental	2nd harmonic	3rd harmonic
Inner race	135.40	270.80	406.20
Outer race	89.60	179.20	268.80
Rolling element	58.87	117.74	176.61

CHARACTERISTICS EXTRACTED THE TIME DOMAIN

1 - RMS Value =	0.010743	2 - Peak Value =	0.026514
3 - Crest Factor =	2.4679	4 - Impulse Factor =	2.7844
5 - Kurtosis =	4.3974		

CHARACTERISTICS OF THE ROLLING BEARING

Item	Name	Value
1-	Ressonance (Hz)	2853
2-	Rotation of the shaft (Hz)	25
3-	Fault Frequency of Inner Race (Hz)	135.5324
4-	Fault Frequency of Outer Race (Hz)	0
5-	Fault Frequency of Rolling elements (Hz)	0
6-	Sampling Frequency (Hz)	10000
7-	Length of the Signal (points)	40000

Figure 13 - The results obtained in the calculation of statistical parameters in the time domain

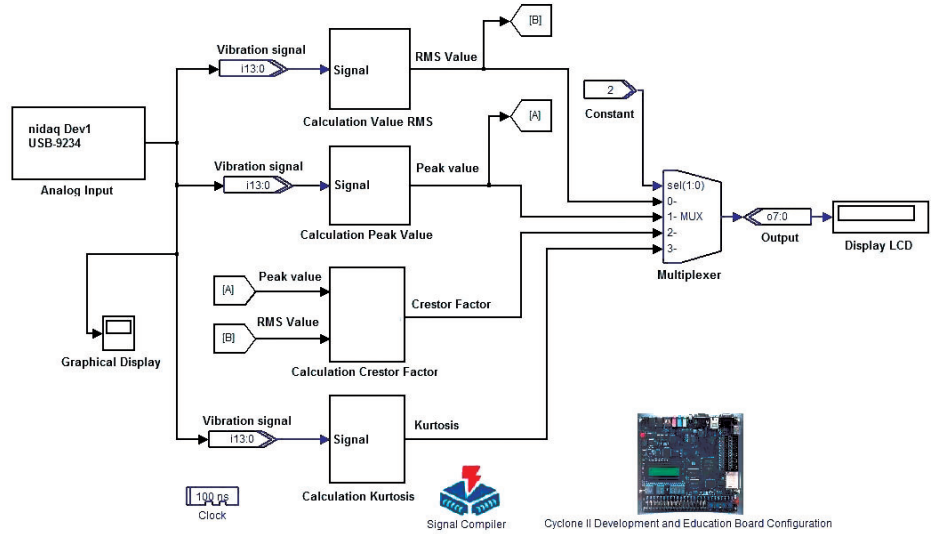

Figure 11 - Block diagram of 2nd stage of instrument modeled in SIMULINK/DSP Builder

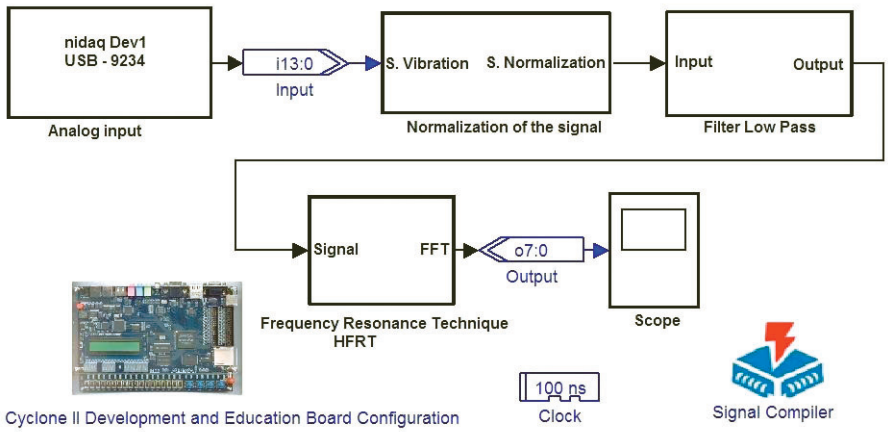

Figure 12 - Block diagram of 3rd stage of instrument modeled in SIMULINK/DSP Builder

Figure 14 shows the time and frequency representations of the vibration signal. In the vibration spectrum presented, the identification of the fault frequency of inner race is not immediate.

Figure 15 shows the results obtained with the high-frequency resonance technique – HFRT by the third stage of the instrument. It shows the spectrum of the vibration signal demodulated with the identification of the five largest amplitude peaks of the spectrum to locate the characteristic frequency of the inner race fault. It can be seen that the relevant frequency component (135. 01Hz) can be easily located.

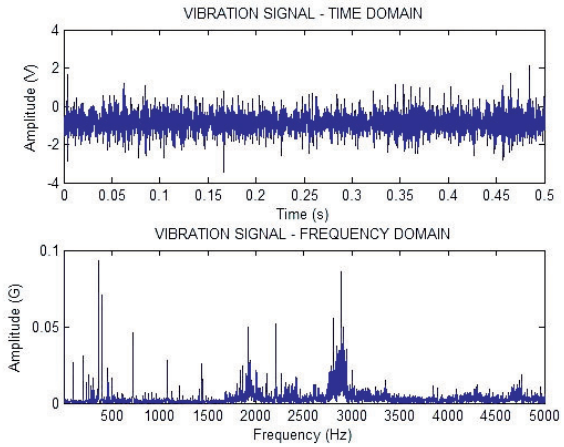

Figure 14 - Vibration signal and the vibration signal spectrum when the bearing inner race has a fault

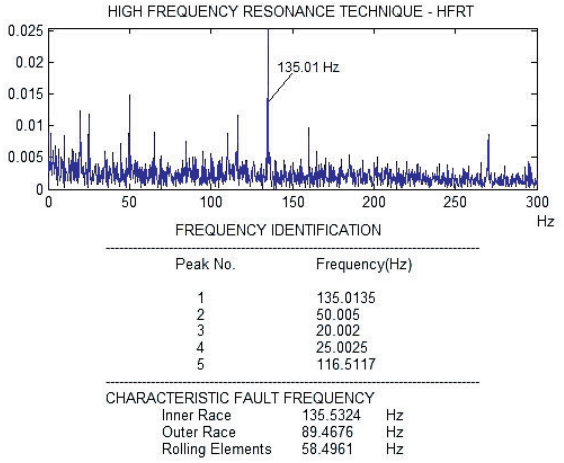

Figure 15 - High-frequency resonance technique with the identification of the characteristic frequency of inner race fault

Figure 16 shows the vibration signal spectrum obtained using the HFRT method to locate the characteristic frequency of the outer race fault (89.50 Hz).

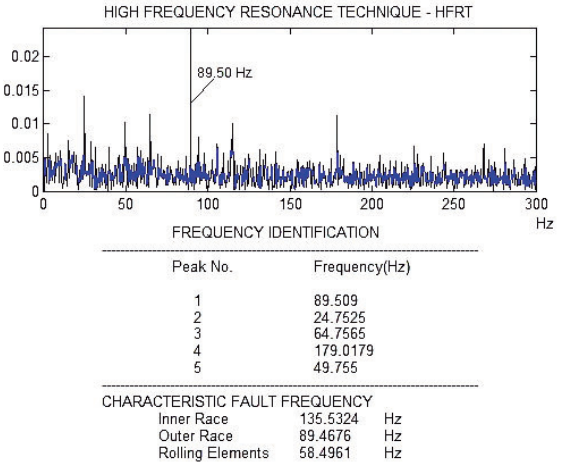

Figure 16 - High-frequency resonance technique with the identification of the characteristic frequency of outer race fault

4 CONCLUSIONS

A complete approach for the modelling, simulation, and development of a real-time vibration measurement and analysis instrument based on a reconfigurable logic, FPGA-based, was developed and tested. The target instrument was capable of identify fault in both inner and outer race of rolling bearings in rotating machines. The results show that the methodology adopted in the proposed project was efficient, facilitating the design flow, with significant reduction of time and costs associated with prototype production. This design flow uses a high-level behavioural description of the DSP algorithm that allows the researcher in a short time develops a new application. The implementation can be simulated and then deployed into an FPGA-based hardware setup.

ACKNOWLEDGMENT

The work developed by Cesar da Costa was sponsored by CAPES/Brazil scholarship.

REFERENCES

[1] M. E. H. Benbouzid, "A review of induction motors signature analysis as a medium for faults detection ", IEEE Transactions on Industrial Electronics, Vol. 47, nº. 5, pp. 984-993, October 2000.

[2] A. Sadoughi, M. Ebrahimi, M. Moalem, S. Sadri," Intelligent diagnosis of broken bars in induction motors based on new features in vibration spectrum". Diagnostic for Electric Machines, Power Electronics and Drives, IEEE International Symposium, pp. 106-111, Sept. 2007.

[3] S. Nandi, H. A. Toliyat, X. Li, "Condition monitoring and fault diagnosis of electrical motors – a review", IEEE Transactions on Energy Conversion, vol. 20, nº. 4, pp. 719-729, Dec. 2005.

[4] S. A. S. Al Kazzas, G.K. Singh, "Experimental investigations on induction machine condition monitoring and fault diagnosis using digital signal processing techniques". Electric Power Systems Research, no. 65, pp. 197-221. New York: Elsevier. 2003.

[5] W. Q. Lim, D. H. Zhang, J. H. Zhou, P. H. Belgi, H. L. Chan, "Vibration – based fault diagnostic platform for rotary machines". IECON 2010 – 36th Annual conference on IEEE Industrial Electrocnics Society, pp. 1404-1409, 2010.

[6] J. J. Rangel- Magdaleno, R. J. Romero- Troncoso, L. M. Contreras-Medina, A. Garcia-Perez. "FPGA implementation of a novel Algorithm for on-line bar breakage detection on induction motors". IEEE International and Measurement Technology Conference, IMTC 2008, pp. 720-725, Canada, 2008.

[7] C. da Costa, M. H. Mathias, P. Ramos, P. S. Girão, "A new approach for real time fault diagnosis in induction motors based on vibration measurement," Proc. Instrumentation and Measurement Technology Conference, Austin, Texas, May 2010, pp. 1164-1168.

[8] C. da Costa, M. Kashiwagi, M. H. Mathias, "Development of an instrumentation system embedded on FPGA for real time measurement of mechanical vibrations in rotating machinery". In: 2012 International Symposium on Instrumentation & Measurement, Sensor Network and Automation (IMSNA), Sanya, China, pp. 60-64, 2012.

[9] A. B. Rey, F. Marin, S. De Pablo, L. C. Herrero, "A methodology for teaching the integrated simulation of power system by modeling with MATLAB/SIMULINK and controlling via a c- based algorithm". Power Electronic Education, 2005, IEEE Workshop, pp. 114-119, 2005.

[10] I. Grout, J. Ryan, T. O´Shea, "Configuration and debug of field programmable gate arrays using Matlab/Simulink", Journal of Physics: Conference Series 15, pp. 244-249, 2000.

[11] M. Zengchui, W.Xin, "Design and realization of real-time spectrum analysis system based on DSP builder". On: 2012 Second International Conference on Instrumentation &, Measurement, Computer, Communication and Control (IMCCC), pp. 1077-1080, 2012.

[12] G. Xiong, X. Zhou, P. Ji, "Implementation of the Quadrature Waveform Generator Based on DSP Builder". IEEE Computer Society, International Symposium on Intelligent Information Technology Application Workshops, IITAW´08, pp. 773-776, Dec. 2008, China.

[13] N. Tandom, A. Choudhury, "A review of vibration and acoustic measurement methods for the detection of defects in rolling element bearings", Tribology International 32, pp. 469-480. New York: Elsevier. 1999.

[14] P. Maedel, Jr, "Vibrations standards and test codes, shock and vibration handbook", 5th edition (Cyril Harris, editor), McGraw Hill Publishing Co., 2001.

[15] A. Lebaroud, G. Clerc, "Diagnosis of induction motor faults using instantaneous frequency signature analysis". IEEE Proceedings of the 2008 International Conference on Electrical Machines, ICEM 2008, 18 th International Conference on, pp. 1-5, Sept. 2008.

[16] J. R. Stack, R. G. Harley, T. G. Habetler, "An amplitude modulation detector for fault diagnosis in rolling element bearing," IEEE Trans. on Industrial Electronics, Vol. 51, Nº. 5, Oct. 2004, pp. 1097-1102.

[17] M. Xiaojian,C. Ruiqi, W. Wenying, "The comparison and application of envelop demodulation in machine fault diagnosis," Journal of DongHua University, Natural Science, Nº. 27, May 2005, pp. 95-97.

[18] A. Sadoughi, H. Behbahanifardl, "A practical bearing fault diagnoser", Proc. International Conference on Condition Monitoring and Diagnosis, Beijing, China, Apr. 2008, pp. 151-154.

[19] F. Pan, S. R. Qin, L. BO, "Development of diagnosis system for rolling bearings faults based on virtual instrument technology," Journal of Physics: Conference Series, International Symposium on Instrumentation Science and Technology, Vol. 48, 2006, pp. 467-473.

[20] P. D. McFadden, J. D. Smith, "Vibration monitoring of rolling element bearings by the high frequency resonance technique – A review". Tribology International, Vol. 17, Issue 1, Feb 1984, pp. 3-10.

[21] H. Prasad, M. Ghosh, S. Biswas, "Diagnostic monitoring of rolling element bearing by high frequency resonance technique", ASLE Transactions, Vol. 28, Issue 4, Mar 2008, pp. 439-448.